INVESTIGATION OF THE REFRIGERATOR BOTTOM CABINET CAVITY ACOUSTIC BEHAVIOR

A Thesis

by

Anıl Öztürk

Submitted to the

Graduate School of Sciences and Engineering

In Partial Fulfillment of the Requirements for

the Degree of

Master of Science

in the

Department of Mechanical Engineering

Özyeğin University

August 2013

INVESTIGATION OF THE REFRIGERATOR BOTTOM CABINET CAVITY ACOUSTIC BEHAVIOR

Approved By:

Assist. Prof. Dr. G. Güven Yapıcı, Advisor
Department of
Mechanical Engineering
Özyeğin University

Assist. Prof. Dr. Özkan Bebek
Department of
Mechanical Engineering
Özyeğin University

Prof. Dr. Haluk Erol
Department of
Mechanical Engineering
Istanbul Technical University

Date of Approval: 01 August 2013

ABSTRACT

This thesis investigates the computational and experimental analysis for the acoustic behavior of a bottom cabinet cavity in a refrigerator. The finite element and analytical approaches are used in order to determine the natural frequencies and associated mode shapes of the bottom cabinet cavity.

The sound of bottom cabinet cavity is related to its frequencies. The noise level of the bottom cabinet, increases at the peak frequencies of the bottom cabinet cavity. The effects of sound propagation from the bottom cabinet of the refrigerator, due to vibration from the compressor in a rectangular cavity, in dictating the overall sound level of the refrigerator is considerable. For the end user, a quiet run is one of the most important criteria in refrigerator selection. Therefore, design of the bottom cabinet cavity, in where the compressor works and causes the noise problem, has a profound significance.

The natural frequencies of the bottom cabinet cavity are investigated. Firstly, natural frequencies are determined with analytical method. Secondly, natural frequencies are determined with numerical analysis using the finite element model of the bottom cabinet cavity. Comparisons with the results of the analytical study verify the validity of the numerical solution. It is seen that finite element model of the bottom cabinet cavity is applicable. Finally, experimental study is carried out for validation of both models. It is seen that the sound pressure of the bottom cabinet of the refrigerator is higher at some frequencies. As a result, these frequencies are in close match with the natural frequencies of the bottom cabinet cavity of the refrigerator which can be determined with the analytical and numerical analysis.

Keywords: Refrigerator, bottom cabinet, acoustic cavity, natural frequency, pressure response, noise control.

ÖZETÇE

Bu tez, bir buzdolabında kabin dibi kavitesinin akustik davranışını sayısal ve deneysel analizlerle incelemektedir. Kabin dibi kavitesinin doğal frekansları ve ilgili mod şekillerini hesaplamak için, analitik ve sonlu elemanlar yaklaşımları kullanılmaktadır.

Kabin dibi kavitesinin sesi frekanslarıyla ilişkilidir. Kabin dibinin gürültü seviyesi ise kavitenin pik frekanslarında artar. Dikdörtgen bir kavite içerisinde titreşimle çalışan kompresörden dolayı, kabin dibinden yayılan sesin, buzdolabının toplam ses seviyesine etkisi önemli derecededir. Buzdolabı seçiminde, sessiz çalışma son kullanıcı için en önemli kriterlerden biridir. Bu yüzden kompresörün çalıştığı ve gürültü problemine yol açan kabin dibi kavitesinin tasarımı büyük bir öneme sahiptir.

Kabin dibi kavitesinin doğal frekansları; öncelikle analitik metot, daha sonra sonlu elemanlar modeli ile nümerik metotlarla bulunmuştur. Analitik çalışmanın sonuçları ile yapılan karşılaştırmalar, nümerik çözümün geçerliliğini doğrulamaktadır ve kabin dibi kavitesinin sonlu elemanlar modelinin uygun olduğu görülmektedir. Son olarak, her iki modelin doğrulanması için deneysel çalışma yapılmıştır. Buzdolabının kabin dibi ses basıncının, bazı frekanslarda daha yüksek olduğu deneysel çalışmada görülmüştür. Sonuç olarak; bu frekansların analitik ve nümerik analizlerle hesaplanabilen buzdolabı kabin dibi kavitesinin doğal frekansları ile yakın olduğu görülmüştür.

Anahtar sözcükler: Buzdolabı, kabin dibi, akustik kavite, doğal frekans, basınç cevabı, gürültü kontrolü.

ACKNOWLEDGMENTS

I would like to express my deepest gratitude and thanks to my advisor, Assist. Prof. Dr. Güney Güven YAPICI, for his continuous support, excellent guidance and valuable advice throughout the progress of this thesis.

I would also like to express my thanks to Prof. Dr. Haluk EROL for his assistance and guidance throughout the experimental study of the thesis.

Finally, I am deeply indebted to my family and friends for their encouragement and continuous support.

Anıl ÖZTÜRK

TABLE OF CONTENTS

ABBREVIATIONS

k	**:** Wave Number	[1/m]
c	**:** Sound Speed	[m/s]
ω	**:** Angular Frequency	[rad/s]
f	**:** Frequency	[Hz]
p	**:** Sound Pressure	[Pa]
FEM	**:** Finite Element Model	
FFT	**:** Fast Fourier Transform	

LIST OF TABLES

LIST OF FIGURES

CHAPTER I

INTRODUCTION

The word "noise" is derived from the Latin word "nausea" which derives from the same word root as seasickness. Noise is unwanted sound that is among the most pervasive pollutants today. Road traffic, airplanes, construction equipment, manufacturing processes, and home appliances, to name a few, are naturally broadcast into the air as indoor and outdoor noise. Noise affects human health and well-being negatively. Problems related to the noise include hearing loss, stress, high blood pressure, sleep loss, distraction and productivity loss, and a general reduction in the quality of life.

Recently, sound comfort or low noise has become important in residential houses. One of the main sources of indoor noise is home appliances. Legislation is becoming more severe on acceptable noise levels and low noise is a major marketing point for many products. Regarding the importance of noise in home appliances, noise emission levels have been added to energy labels.

The European Energy Label shows how efficiently a product uses energy. New products labels rate appliances on a scale from dark green (most efficient) to red (least efficient). The ratings generally go from A to G. However, you may also see higher categories appear in the green bands of A+, A++ and A+++ as products become more energy efficient. For example, energy labels of refrigerators contain power consumption, energy class, volume and noise emission. Figure 1.1 shows a refrigerator energy label [1].

Noise emission is a distinctive feature for the selection of the home appliances in the same energy class. Refrigerators are continuously running when it is compared with other home appliances. Therefore, reduction of refrigerator noise is necessary and noise-free operation becomes the preferred choice of customers in the domestic refrigerators.

This thesis follows the style of *Journal of Sound and Vibration*

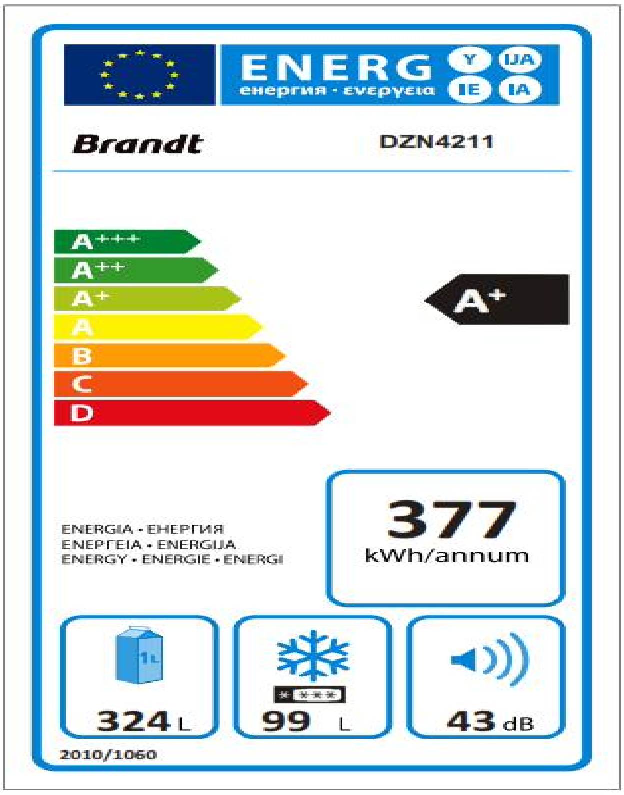

Figure 1.1 A refrigerator energy label

The components in the refrigeration cycle are contributing to the overall noise level. The refrigeration cycle's main components are condenser, expansion valve or capillary tubes, evaporator, fan and compressor. Figure 1.2 shows the components in a typical refrigeration cycle [2].

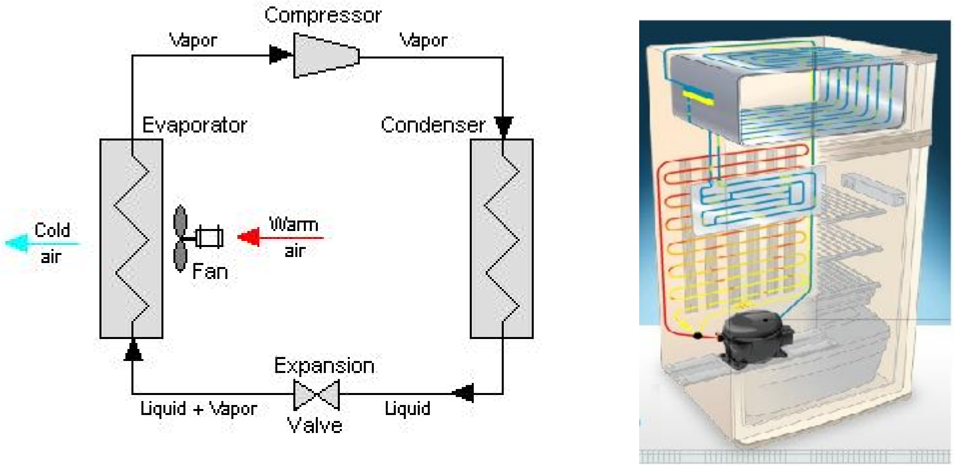

Figure 1.2 Components of a refrigeration cycle

The main role of the condenser is to disperse the heat absorbed by the refrigerant fluid throughout the refrigeration system [3]. The overheated gas in the condenser is releasing heat into the atmosphere; and it is transformed from a gaseous state into a liquid state. The expansion valve or capillary tube is building up resistance to the refrigerant fluid circulation, causing an enormous difference in pressure between the condenser and the evaporator. The refrigerant fluid is still in a liquid state as it passes through the capillary tube towards the evaporator, where it meets with the low pressure. The refrigerant fluid is transformed from liquid state into a gaseous state in the evaporator by absorbing the inside heat of the refrigerator in the process. The compartment with the evaporator contains a fan that provides air circulation, which is shown in Figure 1.3 and comes up to homogenous temperature stratification [4].

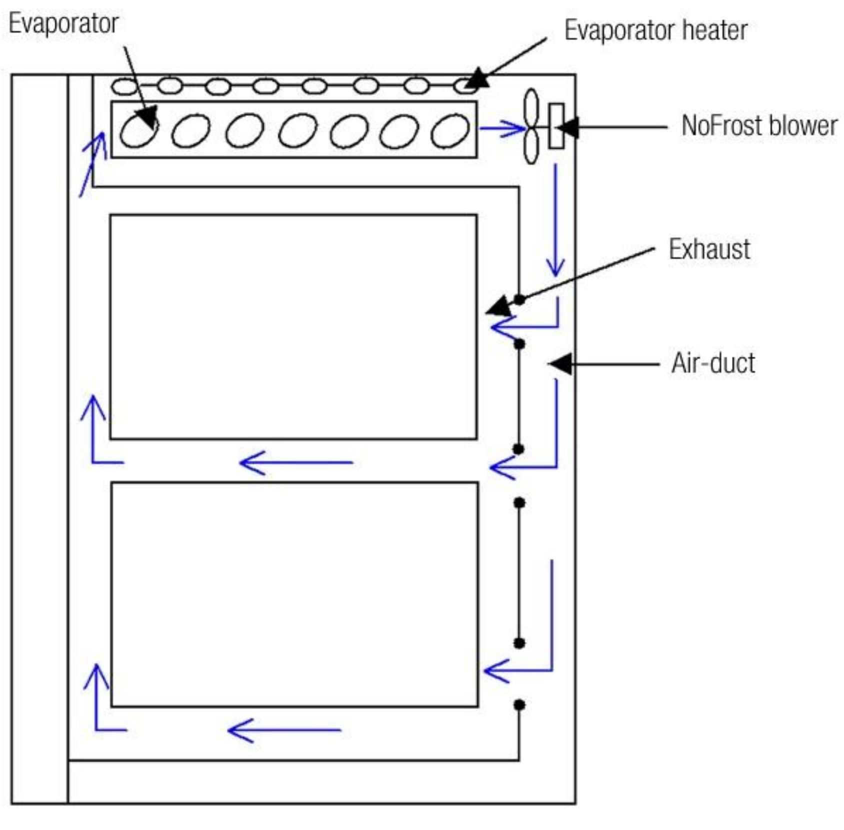

Figure 1.3 Working of a fan in a refrigerator

A compressor pumps the refrigerant fluid, which on returning from the evaporator in a gaseous state, is suctioned and pumped to the condenser. It causes low pressure in the evaporator and high pressure in the condenser, in addition to further elevating the gas temperature.

The compressors in refrigerators are hermetic, reciprocating, direct drive induction motors that are designed with intake and discharge internal mufflers, internal suspension between the crankcase and outer housing, and a flexible steel tube for direct discharge gas to the outside of the housing. The hermetic space contains oil reservoir and the return refrigerant. Figure 1.4 shows the section view of the compressor [5].

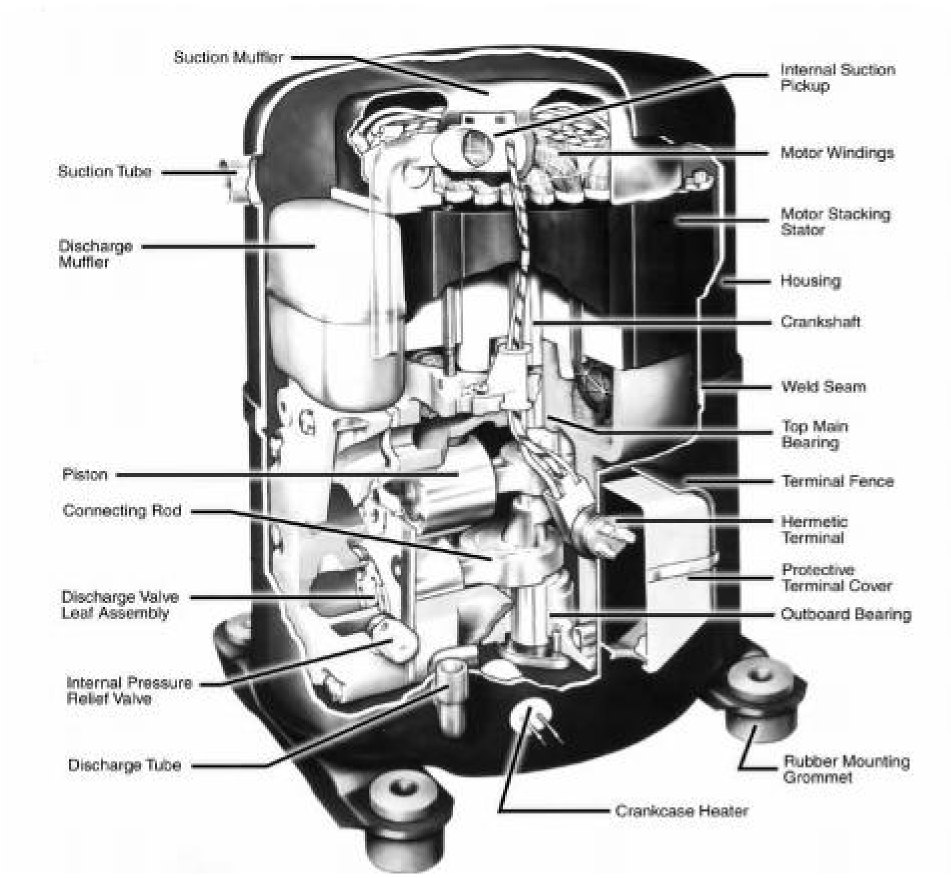

Figure 1.4 The section view of compressor

Together with the fan, the compressor is a source of noise that contributes to most of the refrigerator's overall noise level due to the existence of a rotary element and this element motion creates vibration and noise. Figure 1.5 shows rotary element of the compressor [6].

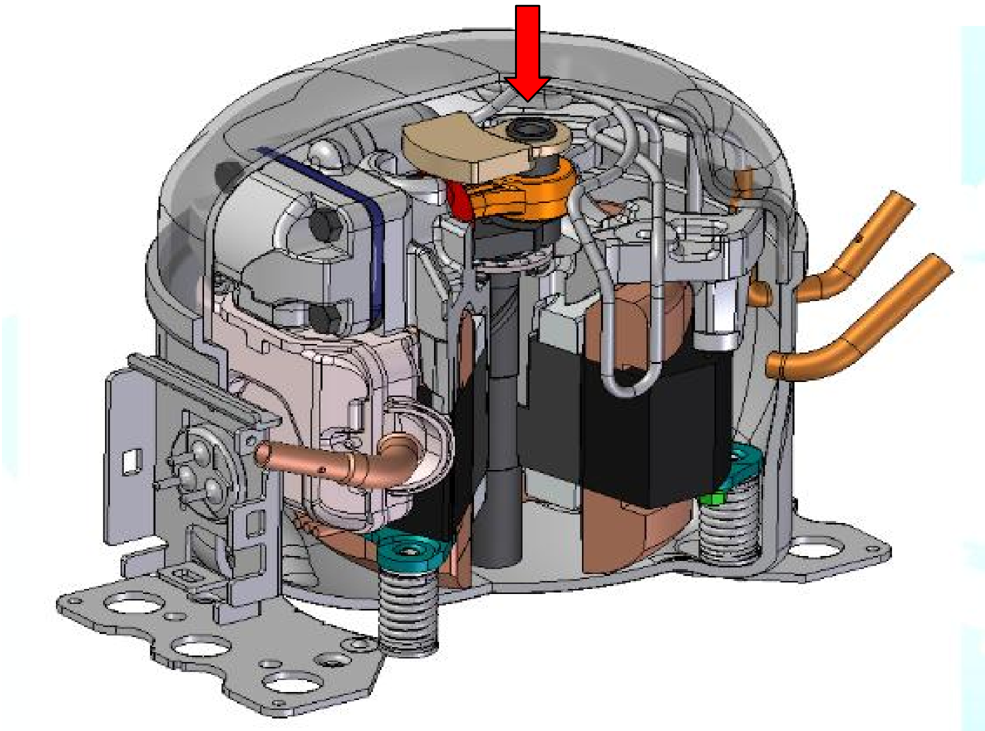

Figure 1.5 The section view of compressor for rotary elements

New designs are expected to be cheaper and meet higher quality standards. Once mass production has started, it is very expensive and difficult to change the design. Therefore, new methods that can quickly respond to the conditions are needed. These methods should reduce engineering costs and must be reliable. Computer-aided engineering has been widely used as a cost-effective solution for testing new designs. The finite element analysis of the system is important in order to control the development cost and time that is related with the design changes before the prototype manufacturing.

Many studies using experimental and/or numerical methods have been carried out on fan or compressor and have contributed to better understanding of the mechanisms of fan or compressor noise generation.

For fans, a detailed review of noise-reduction methods is provided and the main source of aerodynamic tonal noise is shown as the interaction between non-uniform impeller flow and the fixed-volute tongue [7-9]. An experimental study on the source of tonal noise from centrifugal fans is carried out by Velarde-Suárez et al. [10]. They showed that the strong source of noise at the blade-passing frequency is the interaction between the fluctuating flow that leaves the impeller and the volute tongue, and that the source region is concentrated in the vicinity of the volute tongue. Based on this interaction, experiments are performed on the reduction of aerodynamic tonal noise of centrifugal fans by modifying the volute tongue [11].

The propagation and the generation of flow-induced noise in internal flows are quite distinct from flow-induced noise in external flows [12]. From the physical stand-point of sound generation and propagation, acoustic waves that radiate from noise sources in external flows are affected only by interference between the noise sources themselves, whereas waves in internal flows are influenced by interference between the wall and noise sources in addition to interference between the noise sources themselves. Interference between the wall and noise sources leads to modal solutions in internal acoustic fields, such as fan noise in a refrigerator [13]. Therefore, the integral formula is used for predicting the acoustic signal at any location in a duct by combining the modeled sources with Green's function. However, there is no analytic form of Green's function for complicated duct geometries. In this case, inhomogeneous wave equations with modeled source terms are solved by using the boundary element method [14, 15].

For compressors, the behavior of generating noise divided into three frequency bands from its generation mechanism as low frequency band-under (800Hz). Middle frequency band (800Hz-2.5kHz) and high frequency band (above 2.5kHz). The noise in high frequency band is produced by the mechanical transmission between the compressor mechanism and the shell. For this type noise optimization, the clearances in the sliding portion and the stiffness of the component part are attempted to reduce [16]. With regard to middle frequency band, it is generated by fluid noise. Some papers are presented in this region's noise and it is applied to select the suitable place of discharge valve port and to optimize exit shape of the muffler [17]. The path along which the acoustic energy flows the source to the shell is divided in two; the airborne path [18] and the internal solid path between the pump and shell [19-20]. The noise in low frequency band is separated into harmonics of magnetic noise in the motor (250Hz-800Hz) and transmitted noise through mechanical path in a refrigeration system (under 250Hz). The motor noise is tried to be reduced by decreasing the magnetic performance variations or the transmitted noise based on vibration to whole system which include all components separately evaluated [21].

The transmission of noise based on compressor vibration would be modeled by finite element analysis, compared with experimental results [22-23]. The noise due to compressor vibration is related with compressor internal sound field which is in the presence of oil. Thus because of fluid-structure interaction; the transmission of compressor noise is affected. With the decrease of the volume of fluid, the modal frequency of the sound field moves to lower frequencies. With the increase of the housing constraints, the natural frequency of the housing conference shifts [24].

The generated sound by the compressor may be radiated directly or indirectly. Propagation from the steel case is direct type, structure-borne noise by exciting other components of the system is indirect type. So the major paths by which compressor noise is transmitted to the system are the air surrounding the compressor (case radiation), the refrigerant within the tubing discharge pressure pulse, the tubing (discharge and suction lines) and the mounting feet (vibration) [25-26]. These paths are separately evaluated from the point of overall compressor noise and noise reduction for refrigerator can be done by modal component synthesis technique. In some of studies, such a finite element model used to design shell, to uncouple sound sources and structural or cavity modes. A finite element model of the cavity is used, in which cavity's pressure was a modal analysis of the cavity solving Helmholtz equation. The models were tested and validated by means of experimental modal analysis (shell and cavity). Finally, the whole system was validated through measurement of the emitted sound power [27].

In this thesis, acoustic behavior of bottom cabinet cavity in a refrigerator is investigated. The finite element analysis software ABAQUS, analytical method and experimental study are used in order to determine the natural frequencies and associated mode shapes of the bottom cabinet cavity. The following summarizes the aims of this study;

- The natural frequencies of the refrigerator bottom cabinet cavity are determined.
- The mode shapes of the refrigerator bottom cabinet cavity are determined.
- Comparisons with the results of analytical, numerical and experimental studies are carried out and the validity of the numerical solution is verified.
- The peak frequencies of the bottom cabinet of the refrigerator is determined.
- Effect of the bottom cabinet cavity to refrigerator overall noise level is investigated.

CHAPTER II

THEORY AND ANALYTICAL MODELING OF ACOUSTIC BEHAVIOUR IN REFRIGERATOR BOTTOM CABINET CAVITY

2.1 Introduction

The bottom cabinet of the refrigerator contributes to the overall noise due to the presence of compressor, evaporating tray, pipes and a cavity. Figure 2.1 shows a bottom cabinet of refrigerator. The compressor noise has a profound significance on the refrigerator's overall noise, which is transmitted to air from the bottom cabinet cavity.

Figure 2.1 A bottom cabinet of refrigerator

In this thesis, the investigated refrigerator has a 40,5 dBA total sound power level. Figure 2.2 shows total sound power and frequency spectrum of the refrigerator in 1/3 octave band. When the compressor is off, the noise level of the refrigerator decreases to 32,6 dBA. Figure 2.3 shows total sound power and frequency spectrum of the refrigerator without the compressor running. Also, Figure 2.4 shows total sound power and frequency spectrum of the refrigerator without the fan running as 40 dBA. According to these results, it is seen that the bottom cabinet of the refrigerator has a profound significance on the refrigerator's overall noise.

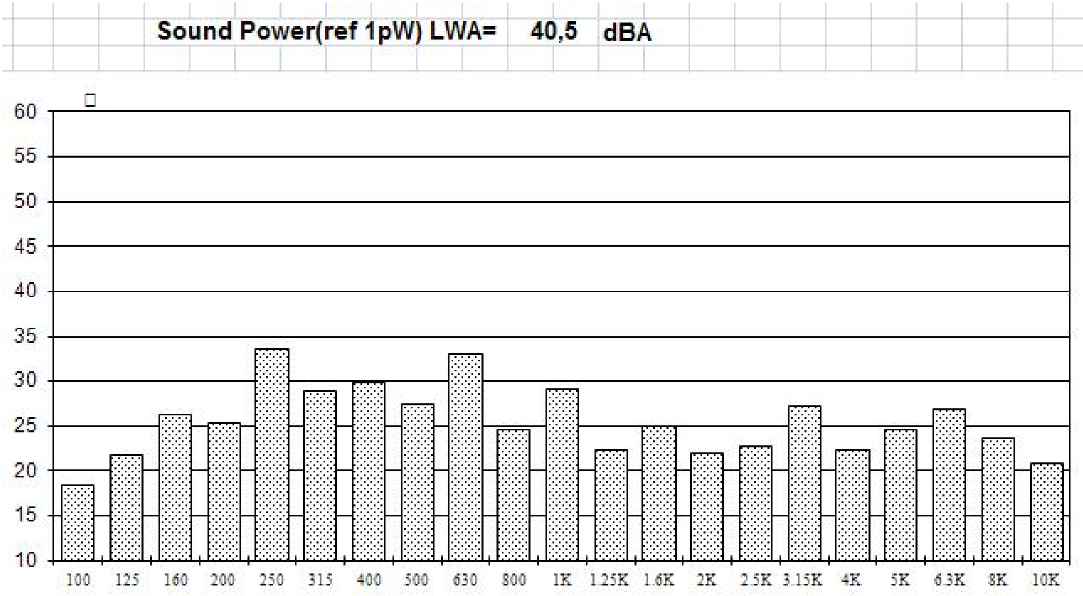

[Hz]	100	125	160	200	250	315	400	500	630	800	1K	1.25K	1.6K	2K	2.5K	3.15K	4K	5K	6.3K	8K	10K	LW
[dB]	37,4	37,9	39,6	36,2	42,2	35,5	34,7	30,6	35,0	25,4	29,0	21,8	24,0	20,8	21,3	26,0	21,3	24,1	27,0	24,7	23,3	**47,5**
[dBA	18,3	21,8	26,2	25,3	33,6	28,9	29,9	27,4	33,1	24,6	29,0	22,4	25,0	22,0	22,6	27,2	22,3	24,6	26,9	23,6	20,8	**40,5**

Figure 2.2 Total sound power of investigated refrigerator

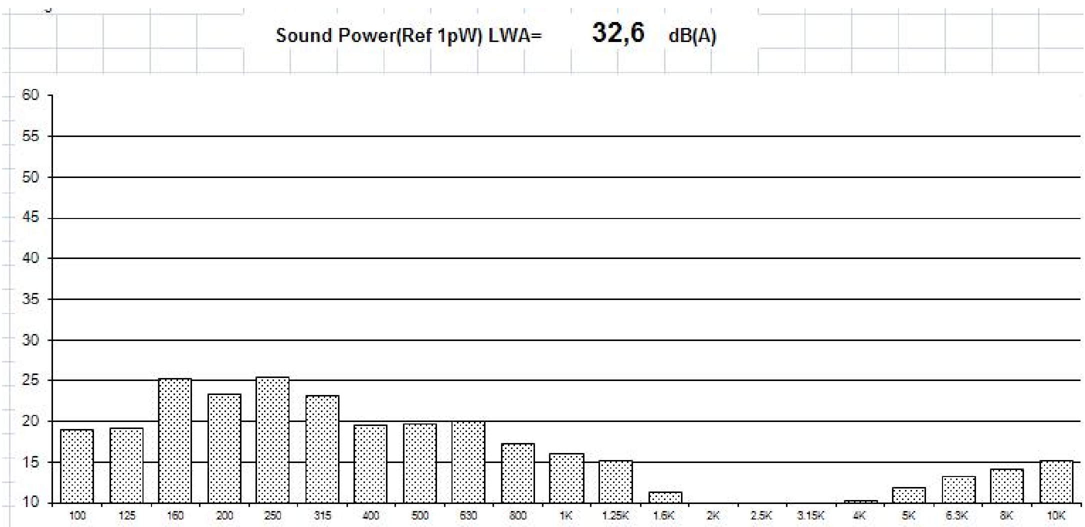

[Hz]	100	125	160	200	250	315	400	500	630	800	1K	1.25K	1.6K	2K	2.5K	3.15K	4K	5K	6.3K	8K	10K	LWA
[dBA]	19,0	19,2	25,2	23,3	25,5	23,2	19,5	19,6	20,1	17,2	16,0	15,1	11,3	7,2	6,5	8,9	10,3	11,8	13,2	14,0	15,2	32,6

Figure 2.3 Total sound power of refrigerator without compressor running

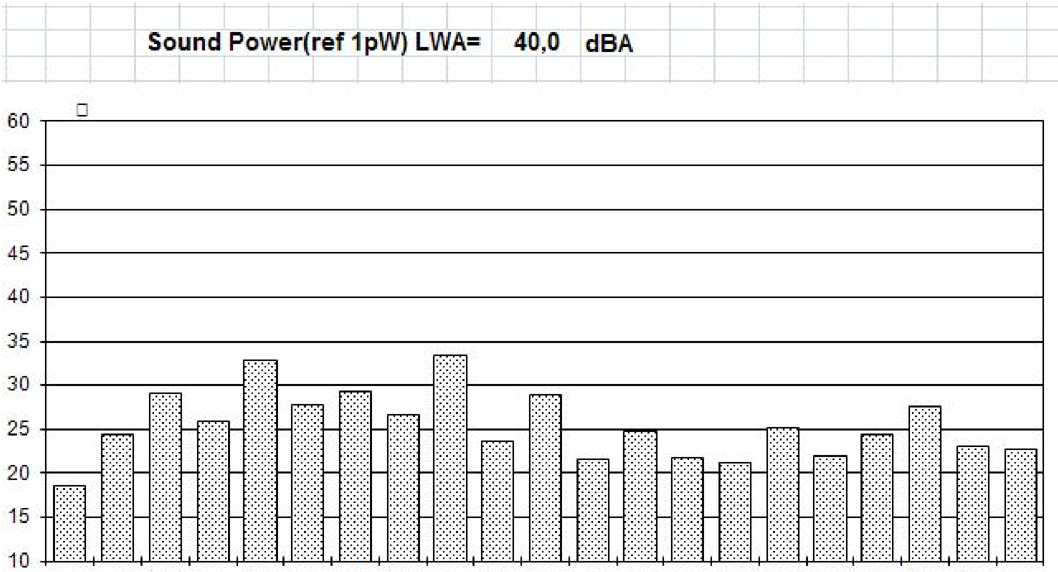

[Hz]	100	125	160	200	250	315	400	500	630	800	1K	1.25K	1.6K	2K	2.5K	3.15K	4K	5K	6.3K	8K	10K	LW
[dBA]	18,6	24,3	29,0	25,8	32,8	27,8	29,2	26,6	33,4	23,7	28,8	21,5	24,8	21,8	21,1	25,2	22,0	24,3	27,6	23,0	22,6	40,0

Figure 2.4 Total sound power of refrigerator without fan running

2.2 Theory

Vibration of structures is one of the main causes of interior noise in cavities. The cavities are closed regions of space that have confinement acoustic energy. Standing waves are stimulated in non-enclosed spaces. The normal modes associated with the standing waves are used to determine acoustic behavior of cavities. Accurate modeling is required in eigenfrequency analysis.

Consider a rectangular cavity of dimensions L_x, L_y, L_z as indicated Figure 2.5. This box represents the refrigerator bottom cabinet. Assume that all surfaces of the cavity are perfectly rigid so that the normal component of the particle velocity vanishes at all boundaries [28].

$$\left(\frac{\partial p}{\partial x}\right)_{x=0} = \left(\frac{\partial p}{\partial x}\right)_{x=L_x} = 0$$
$$\left(\frac{\partial p}{\partial y}\right)_{y=0} = \left(\frac{\partial p}{\partial y}\right)_{y=L_y} = 0 \qquad (2.2.1)$$
$$\left(\frac{\partial p}{\partial z}\right)_{z=0} = \left(\frac{\partial p}{\partial x}\right)_{z=L_z} = 0$$

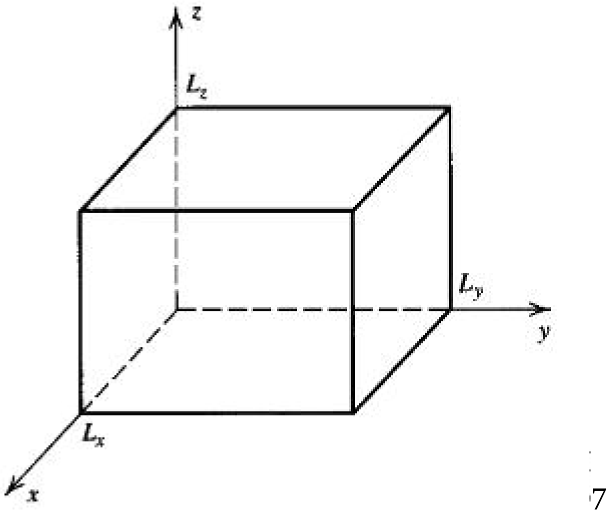

Figure 2.5 The rectangular cavity with dimensions $L_{x,}$ L_y, L_z

Wave equation in three dimension in general;

$$\frac{\partial^2 p}{\partial x^2} + \frac{\partial^2 p}{\partial y^2} + \frac{\partial^2 p}{\partial z^2} = \frac{1}{c^2}\frac{\partial^2 p}{\partial t^2} \qquad (2.2.2)$$

Equation 2.2.2 may be expressed in more general form;

$$\nabla^2 p = \frac{1}{c^2}\frac{\partial^2 p}{\partial t^2} \qquad (2.2.3)$$

Where ∇^2 is the Laplacian operator and three-dimensional wave equation;

$$\nabla^2 = \frac{\partial^2}{\partial x^2} + \frac{\partial^2}{\partial y^2} + \frac{\partial^2}{\partial z^2} \qquad (2.2.4)$$

It is conventional to assume the solutions have the form;

$$p = \Psi e^{iwt} \qquad (2.2.5)$$

where Ψ is the function of pressure. Substitution and identification of k = w/c yields the Helmholtz equation.

$$\nabla^2\Psi + k^2\Psi = 0 \tag{2.2.6}$$

Since acoustic energy cannot escape from a closed cavity with rigid boundaries appropriate solutions of the wave equation are standing waves. Boundary conditions are written for this rectangular cavity that has 6 rigid surfaces like this;

Rigid surfaces; *x = 0, x = Lx and y= 0, y = Ly, and z = 0, z = Lz*

$$p(0,y,z.t) = p(L_x,y,z,t) = p(x,0,z,t) = p(x,L_y,z,t) = p(x,y,0,t) = p(x,y,L_z,t) = 0 \tag{2.2.7}$$

Assuming a solution

$$p\,(x,y,z,t)= \Psi\,(x,y,z)\,e^{iwt} \tag{2.2.8}$$

to Eq. (2.2.3) gives

$$\frac{\partial^2\Psi}{\partial x^2} + \frac{\partial^2\Psi}{\partial y^2} + \frac{\partial^2\Psi}{\partial z^2} + k^2\Psi = 0 \tag{2.2.9}$$

Now, apply the method of separation of variables by assuming that Ψ is the product of three functions, each dependent on only one of dimensions,

$$\Psi\,(x,y,z) = X(x)\,Y(y)\,Z(z) \tag{2.2.10}$$

Substitution and division by = X(x)Y(y)Z(z) gives

$$\frac{1}{X}\frac{d^2X}{dx^2} + \frac{1}{Y}\frac{d^2Y}{dy^2} + \frac{1}{Z}\frac{d^2Z}{dz^2} + k^2 = 0 \tag{2.2.11}$$

Since the first term is a function only of x, second only of y and third only of z, all must be constants; otherwise the four terms cannot sum to zero for all x, y and z. This provides the trio of equations

$$\frac{d^2X}{dx^2} + k_x{}^2X = 0\,,\ \frac{d^2Y}{dy^2} + k_y{}^2Y = 0\,,\ \frac{d^2Z}{dz^2} + k_z{}^2Z = 0 \tag{2.2.12}$$

where the constants k_x, k_y and k_z are related by

$$k_x{}^2 + k_y{}^2 + k_z{}^2 = k^2 \tag{2.2.13}$$

Solutions are sinusoids, so that

$$y\left(x,y,z,t\right) = A\sin(k_x x + ¤_x)\sin(k_y y + ¤_y)\sin(k_z z + ¤_z)e^{j\mu t} \tag{2.2.14}$$

where k_x,k_y,k_z,$ø_x$,$ø_y$, and $ø_z$ are determined by the boundary conditions. These conditions *p(0,y,z.t) ,p(x,0,z,t) and p(x,y,0,t)* require ,$ø_x = 0$, $ø_y = 0$ and $ø_z = 0$, and $p(L_x,y,z,t) = p(x,L_y,z,t) = p(x,y,L_z,t) = 0$ require the arguments k_xL_x , k_yL_y and k_zL_z to be integral multiples of π. Thus, the standing waves on the rectangular cavity becomes

$$p_{lmn} = A_{lmn} cos\ k_{xl} x\ cos\ k_{ym} y\ cos\ k_{zn} z\ e^{iw_{lmn} t} \tag{2.2.15}$$

where the components of k are

$$\begin{aligned} k_{xl} &= l® \ / \ L_x \qquad l = 0,\ 1,\ 2,\ldots \\ k_{ym} &= m® \ / \ L_y \qquad m = 0,\ 1,\ 2,\ldots \\ k_{zn} &= n® \ / \ L_z \qquad n = 0,\ 1,\ 2,\ldots \end{aligned} \tag{2.2.16}$$

A is the maximum displacement amplitude, these equations limit the wave numbers k_x , k_y and k_z to discrete sets of values, which in turn restrict the natural frequencies for the allowed modes to

$$f_{lmn} = c\ /\ 2\ \left[\left(l\ /\ L_x \right)^2 + \left(m\ /\ L_y \right)^2 + \left(n\ /\ L_z \right)^2 \right]^{1/2} \tag{2.2.17}$$

Thus, the allowed angular frequencies of vibration are quantized,

$$\boldsymbol{\omega}_{lmn} = c\left[\left(l®\ /\ L_x \right)^2 + \left(m®\ /\ L_y \right)^2 + \left(n®\ /\ L_z \right)^2 \right]^{1/2} \tag{2.2.18}$$

Equation (2.2.15) has its own angular frequency and can be specified by the ordered integers (l,m,n), gives three-dimensional standing waves in the cavity with nodal planes parallel to the walls. Between these nodal planes, the pressure varies sinusoidal, with the pressure within a given loop in phase, and with adjacent loops 180° out of phase.

If only those modes for which n = 0 are considered, the z component of the propagation vector vanishes, and the resulting standing wave patterns become two-dimensional.

A rigid boundary for a pressure wave in a fluid is analogous to a free boundary for a membrane displacement wave in that both correspond to respective antinodes. The distribution of nodes and antinodes of these respective pressure and displacement waves in planes perpendicular to any axis will be identical for the same dimensions and modal numbers [28].

2.3 Analytical Model

An analytical model is used for studying the acoustic behavior of cavity in a refrigerator bottom cabinet. Figure 2.6 shows the refrigerator bottom cabinet cavity in L_x, L_y, L_z dimensions. An approach to this model is to consider an enclosure with six rigid boundary conditions. The enclosure is a rectangular box shaped bottom cabinet cavity that must be model by standing waves on the rectangular cavity (2.2.15). By using k components equation (2.2.16), eigenfrequencies and mode shapes can be determined by equation (2.2.18).

For this analytical model, solution has been provided in Wolfram Mathematica with a workstation which has Intel Xenon Processor E5506 QC 2.13 GHz, 1066 Mhz memory, Quad-Core, 24 Gb Ram.

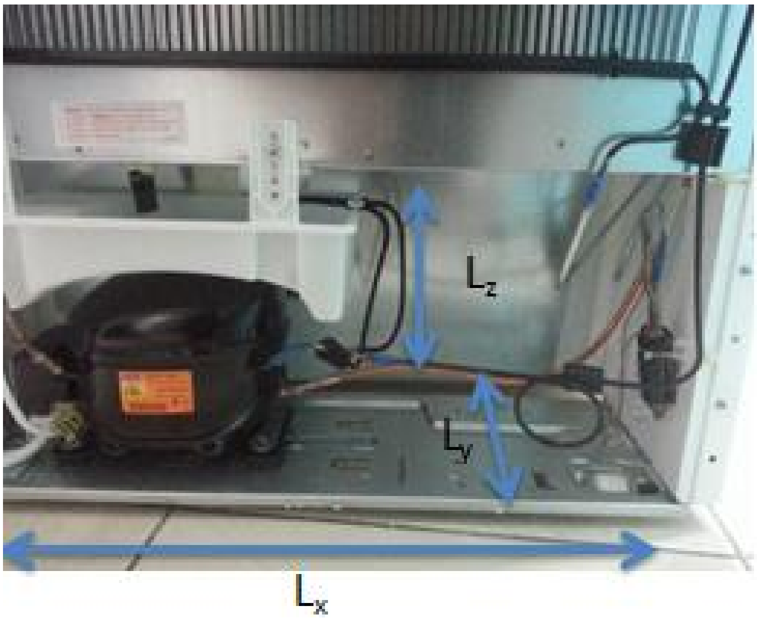

Figure 2.6 Refrigerator Bottom Cabinet in $L_{x,}$ $L_{y,}$ L_z dimensions

The investigation of the refrigerator bottom cabinet cavity which has rectangular shape has been done for dimensions L_x = 0.6m, L_y = 0.3m, L_z = 0.25m as indicated Figure 2.6.

For determining of the angular frequencies in Mathematica, equation (2.2.18) is used as follows;

$$
\begin{aligned}
&k = \sqrt{(\frac{x®}{0.6})^2 + (\frac{y®}{0.3})^2 + (\frac{z®}{0.25})^2} \\
&\boldsymbol{\omega} = c \cdot k \\
&\boldsymbol{\omega} = 2® f \\
&Do[Print[\boldsymbol{\omega}],\{l,1,8,1\},\{m,1,8,1\},\{n,1,8,1\}]
\end{aligned}
\qquad (2.2.19)
$$

where l,m,n are mode numbers between 0 and 8, c is the sound speed in air as 343.8 m/s

For determining mode shapes in Mathematica, pressure equation (2.2.15) is used as follows;

$$
ContourPlot3D[Cos[\frac{3.14x*l}{0.6}]Cos[\frac{3.14y*m}{0.3}]Cos[\frac{3.14z*n}{0.25}],\{x,0,0.6\},\{y,0,0.3\},\{z,0,0.25\}] \qquad (2.2.20)
$$

As a result, the natural frequencies and mode shapes of the acoustical system obtained by assuming that the boundaries of the enclosure are hard, hence the pressure gradients on all boundaries are set to zero.

Figure 2.7 shows a few mode shapes of the bottom cabinet cavity in analytical model.

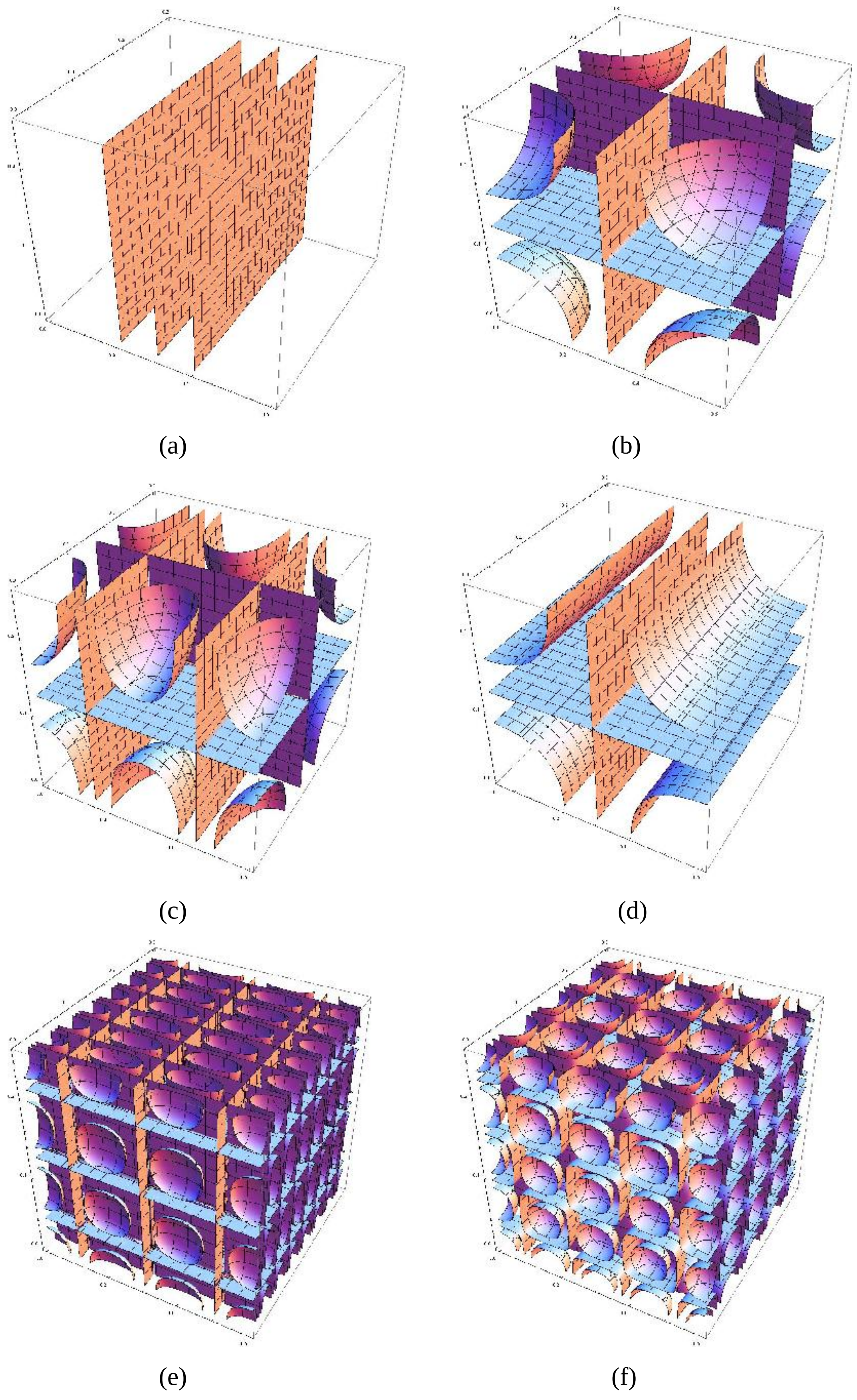

Figure 2.7 A few mode shapes of the bottom cabinet cavity in analytical model

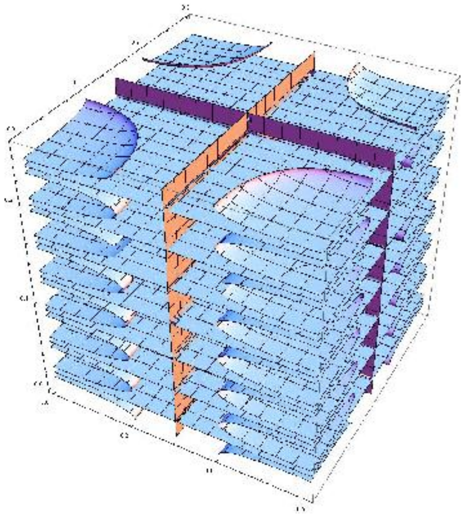

(g)

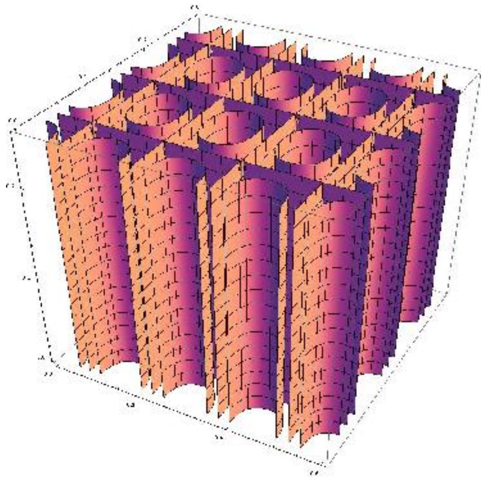

(h)

Figure 2.7 A few mode shapes of the bottom cabinet cavity in analytical model (Continued)

Table 2.1 lists that some of the natural frequencies (Hz) of the bottom cabinet cavity with analytical solution.

Table 2.1 Some of the natural frequencies (Hz) of the bottom cabinet cavity with Analytical Solution

Mode Number (l,m,n)	Frequency	Figure Description
1,0,0	285,88	(a)
1,1,1	937,77	(b)
2,1,1	1060,48	(c)
1,0,1	743,3	(d)
3,7,3	4581,66	(e)
4,4,4	3751	(f)
1,1,7	4845.22	(g)
4,3,0	2061,55	(h)

CHAPTER III

FINITE ELEMENT ANALYSIS

This section describes the three-dimensional finite element models and analysis of bottom cabinet cavity in refrigerator. The natural frequencies and mode shapes of cavity are determined by ABAQUS finite element analysis software. The importance of developing the finite element model is to be able to utilize it in complex models that cannot solved analytically.

3.1 Finite Element Model

Finite element model of a rectangular cavity in L_x = 0.6m, L_y = 0.3m, L_z = 0.25m dimensions is developed by using three-dimensional design software Creo 2.0. It is imported to the ABAQUS finite element analysis software in order to determine the natural frequencies and associated mode shapes. Figure 3.1 shows the bottom cabinet cavity model in ABAQUS.

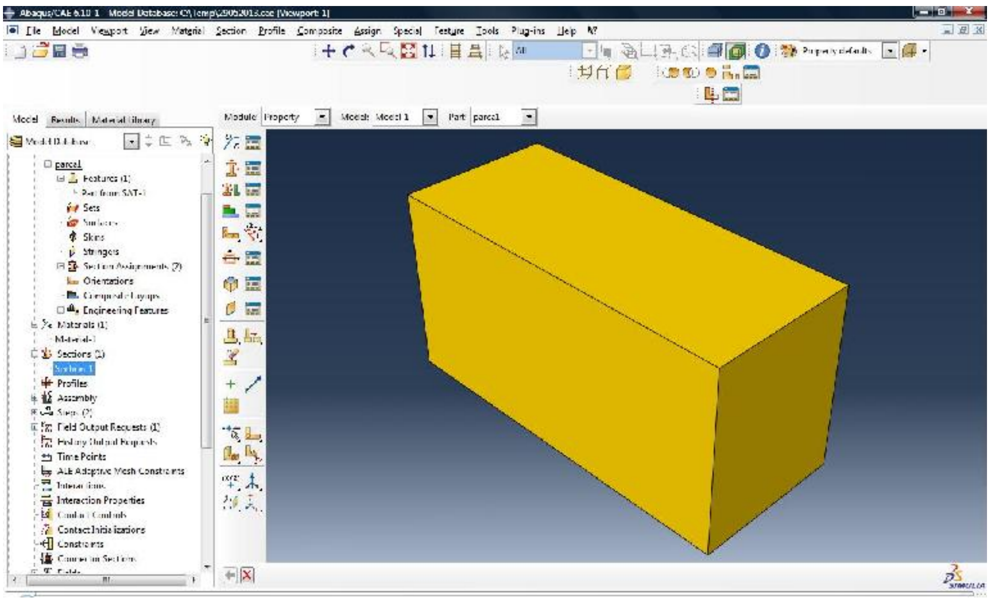

Figure 3.1 Bottom Cabinet Acoustic Cavity Model in ABAQUS

In cavity analysis, “acoustic medium”, “mass density” and “bulk modulus” are critical specifications in material definition, When the acoustic medium property and bulk modulus are not defined correctly, the results of analysis will be wrong.

A material defined as air that has $1.01*10^5$ Pa bulk modulus and 1.226 kg/m^3 density at ambient temperature. Figure 3.2 shows definition of the material.

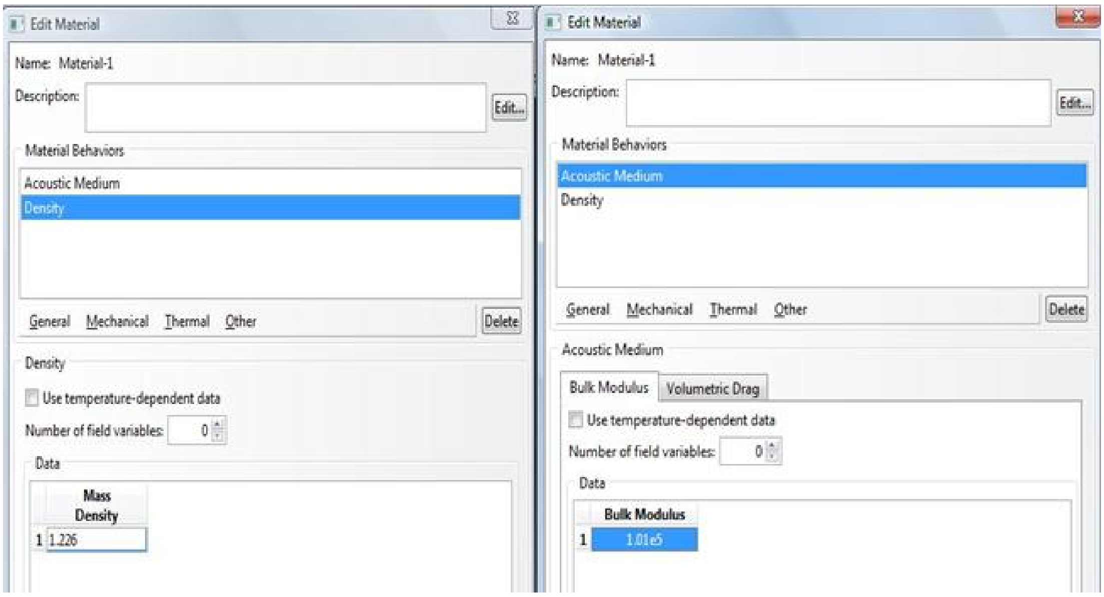

Figure 3.2 Definition of material

The element size has a major significance on the accuracy of the finite element results. In case of the element size decreasing, accuracy of the finite element analysis results increases; but at the same time, the solution time increases with that. Herein, selection of the element size, which gives high accuracy with the minimum solution time is important. Figure 3.3 shows the nodes which are arranged to represent the geometry.

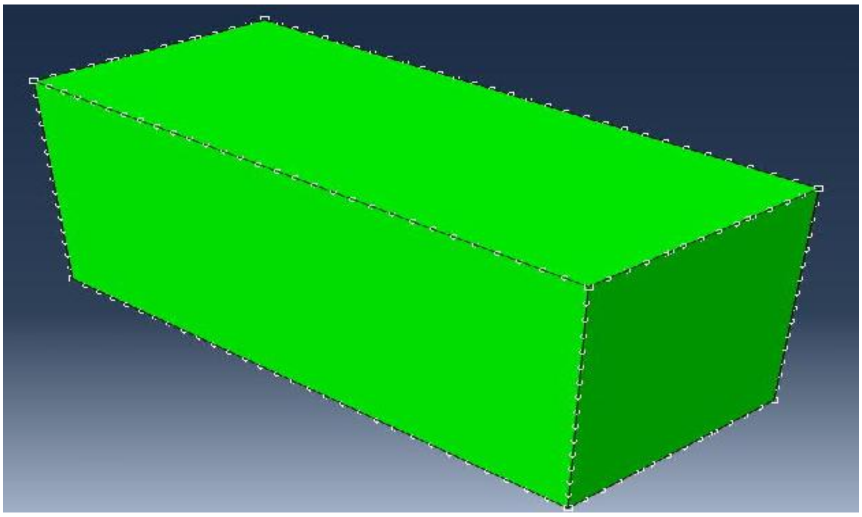

Figure 3.3 Arranging of nodes in geometry

After placement of the nodes; the mesh element type is chosen as acoustic and hex element type. Choosing acoustic element type is very important for correct results. Figure 3.4 shows mesh element type selection.

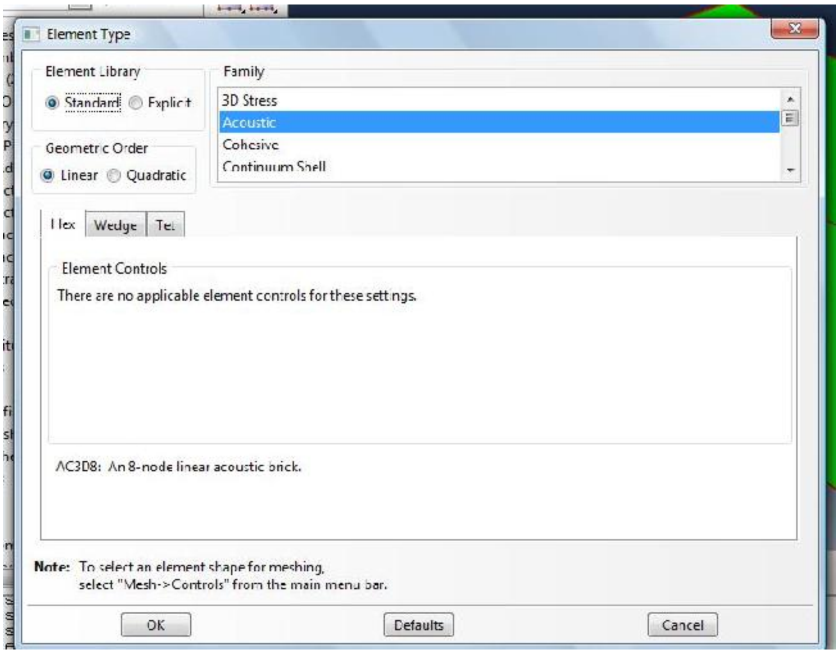

Figure 3.4 Mesh Element Type

Figure 3.5 shows the generated mesh model. The bottom cabinet cavity model consists of 6214 mesh elements in hex shape and 20mm size. The aspect ratio is 1,04.

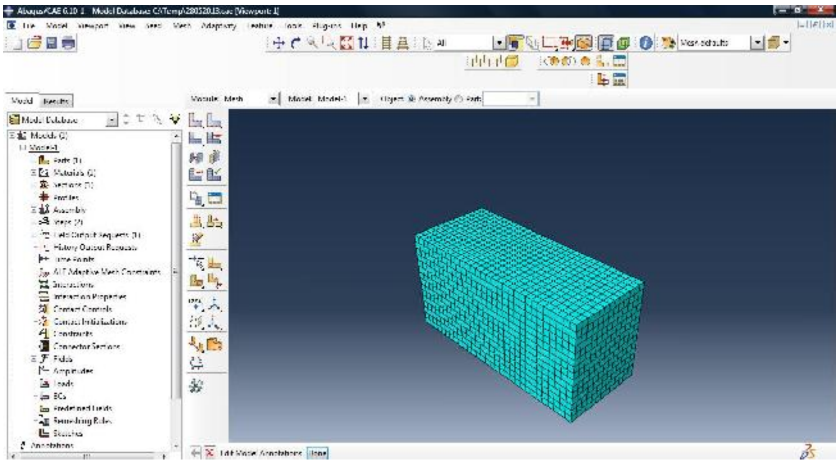

Figure 3.5 Mesh Generation

The solution is provided with linear perturbation procedure type and Lanczos eigensolver in order to determine natural frequencies and modes shapes. Figure 3.6 shows selection of solution procedure. Solution time is 60.28 seconds.

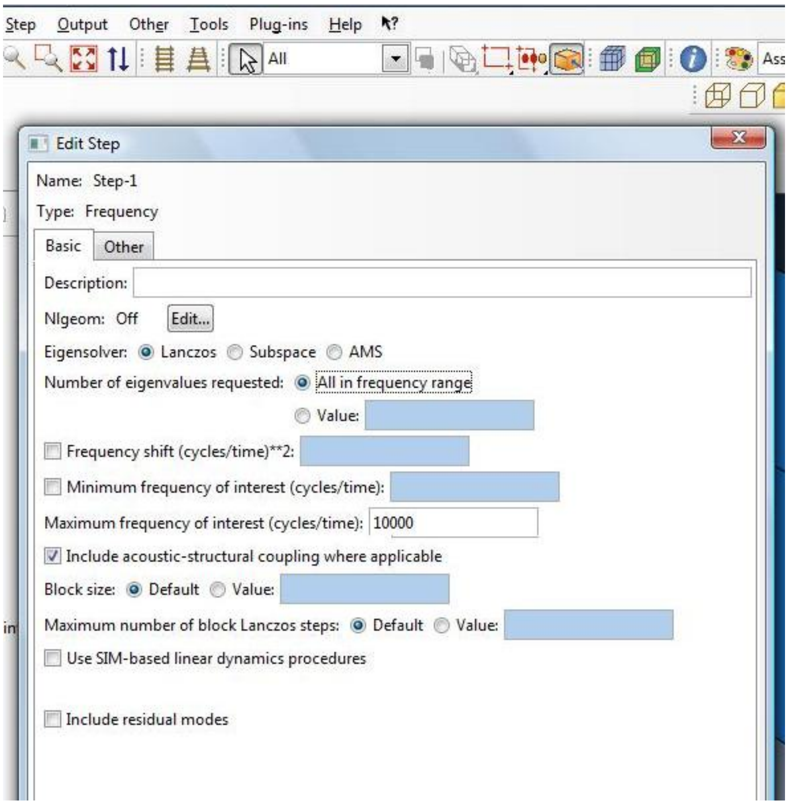

Figure 3.6 Selection of solution procedure

As a result, the natural frequencies and mode shapes of the acoustical system are obtained by ABAQUS finite element analysis simulation software. Figure 3.7 shows a few mode shapes of the bottom cabinet acoustic cavity in ABAQUS.

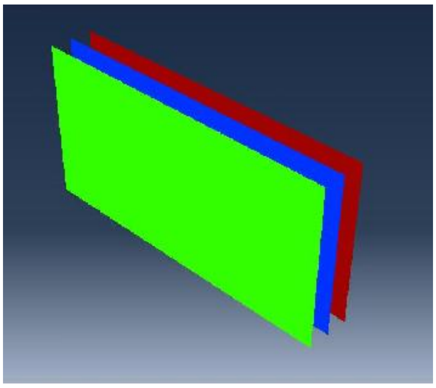

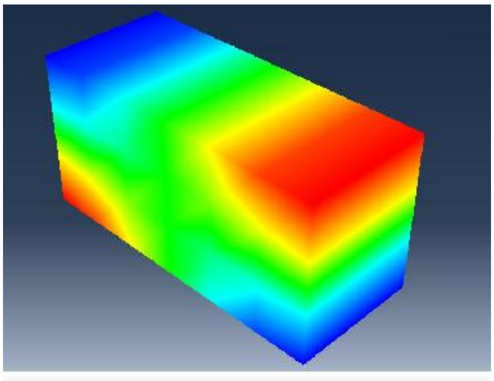

(i) (j)

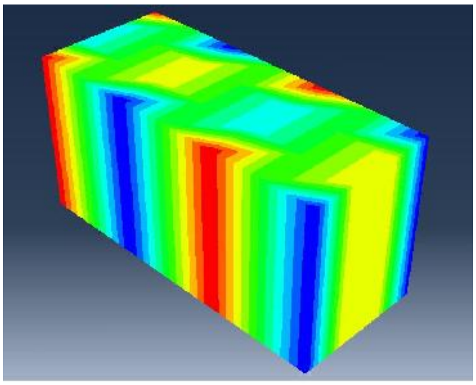

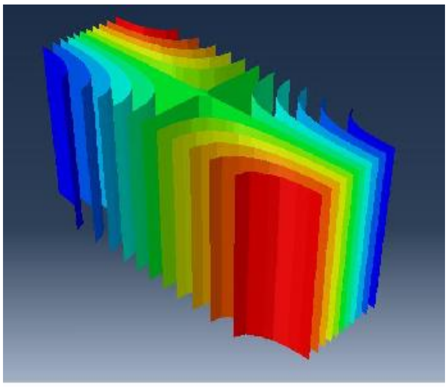

(k) (l)

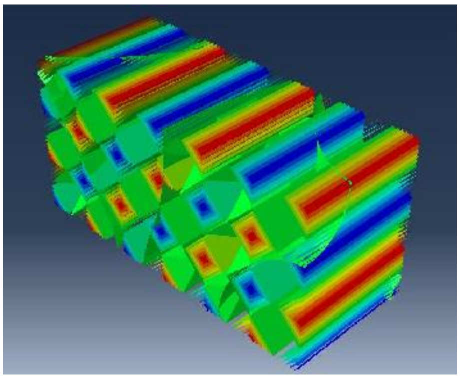

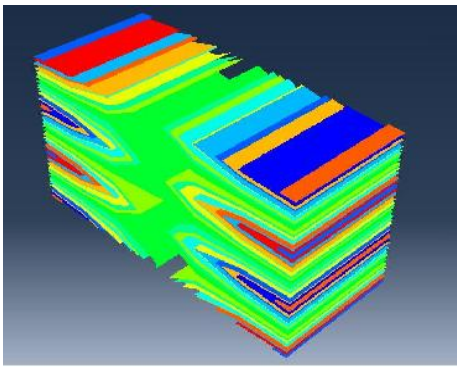

(m) (n)

Figure 3.7 A few mode shapes of the bottom cabinet acoustic cavity in ABAQUS

When element size is changed to 15mm from 20mm for the bottom cabinet cavity model, the mesh elements are increasing to 13600. Solution time is 82.40 seconds. Table 3.1 lists some of natural frequencies of the bottom cabinet cavity with numeric analysis for 20mm and 15mm element size.

Table 3.1 Some of the natural frequencies (Hz) of the bottom cabinet cavity with Numeric Analysis

Mode Number (l,m.n)	Frequency element size 20mm	Frequency element size 15mm	Figure Description
0,1,0	571,42	571,51	(i)
1,0,1	746,62	745,5	(j)
3,2,0	1427,42	1428,35	(k)
1,1,0	643,26	643,6	(l)
6,0,2	2200,12	2198,87	(m)
1,0,3	2088,28	2086,77	(n)

3.2 Comparison of FEM Model and Analytical Model

The natural frequencies of the cavity were computed from the FEM model and they are compared with the analytical model. Table 3.2 lists the comparison of the first seven eigenfrequencies between finite element model with analytical model for the different element sizes.

Table 3.2 Comparison of the first seven eigenfrequencies between finite elemet model with analtical results for the bottom cabinet acoustic cavity.

Mode (l,m,n)	Analytical	Numerical element size 100mm	Numerical element size 50mm	Numerical element size 30mm	Numerical element size 20mm	Numerical element size 15mm	Numerical element size 10mm
(1,0,0)	285,88	288,94	287,63	286,46	285,67	285,72	285,78
(0,1,0)	571,77	573,27	572,86	572,1	571,42	571,51	571,6
(1,1,0)	639,25	647,78	645,23	644,5	643,26	643,6	643,25
(0,0,1)	686,12	716,3	710,54	704,87	700,42	699,65	699,1
(1,0,1)	743,3	770,26	760,38	754,28	746,62	745,5	744,8
(0,1,1)	893,13	924,87	918,78	909,38	904,64	902,73	901,45
(1,1,1)	937,77	955,2	954,62	943,67	938,57	934,21	934,96

Mode shapes of the cavity FEM model are also compared with analytical model. Figure 3.8 shows comparison of a few mode shapes in ABAQUS with analytical for the bottom cabinet cavity.

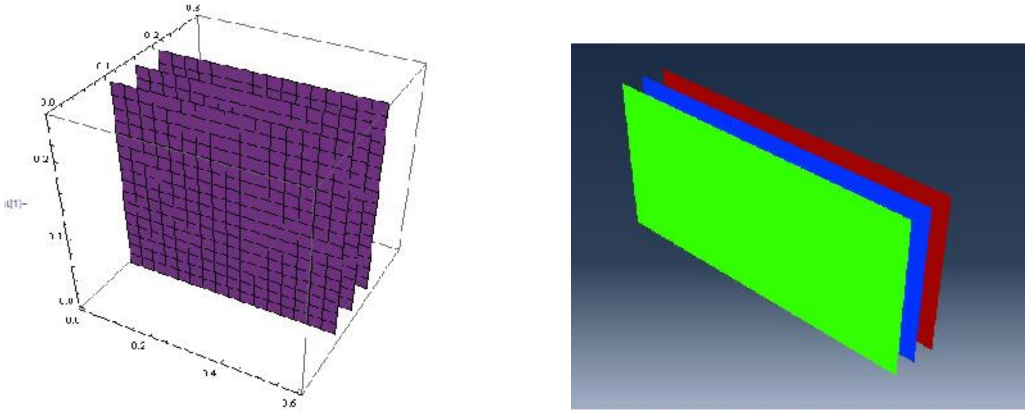

(0,1,0 mode)

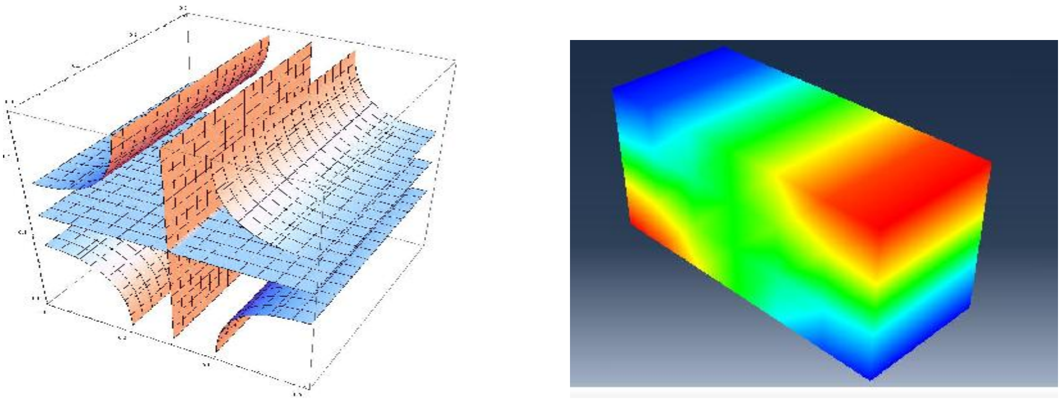

(1,0,1 mode)

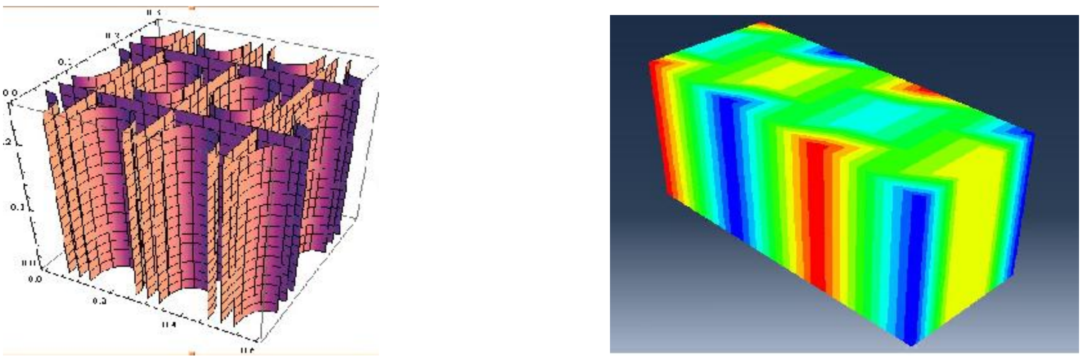

(3,2,0 mode)

Figure 3.8 Comparison of a few mode shapes in ABAQUS with analytical for the bottom cabinet cavity

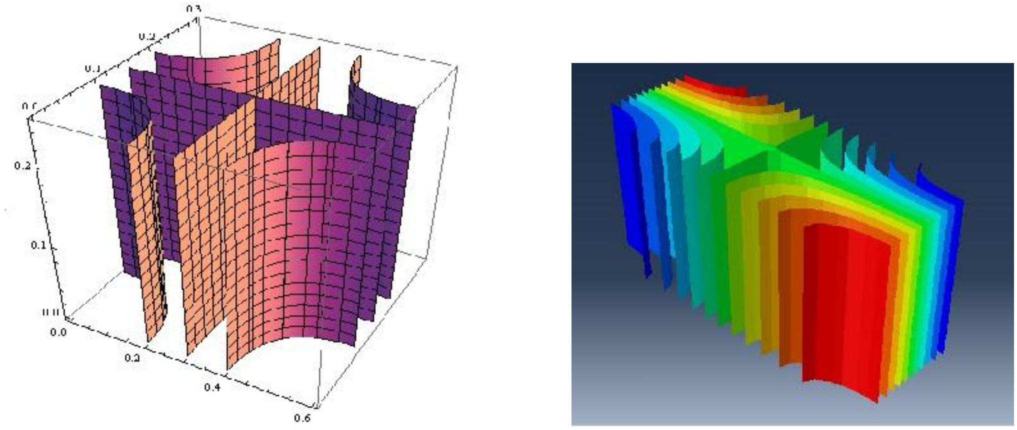

(1,1,0 mode)

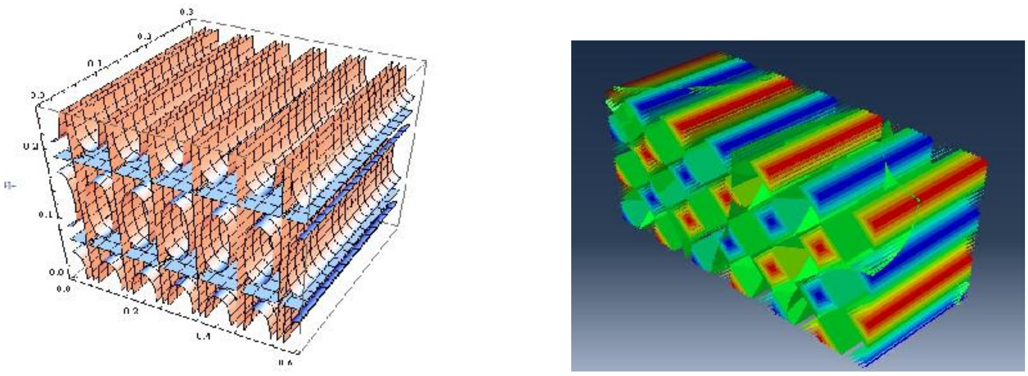

(6,0,2 mode)

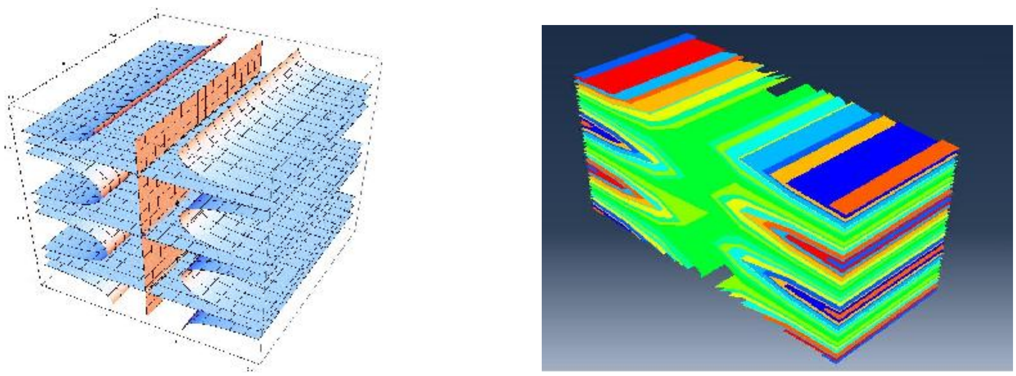

(1,0,3 mode)

Figure 3.8 Comparison of a few mode shapes in ABAQUS with analytical for the bottom cabinet cavity (Continued)

Table 3.3 shows the comparison of the first seven eigenfrequencies mean errors between finite element model with the analytical results for the bottom cabinet acoustic cavity in different generated mesh element sizes. A remarkable change in results is obtained when decreasing the element sizes of the mesh from 100mm to 20mm. Meanwhile, the change in natural frequency obtained with 10mm element sizes in comparison with 20mm is negligible. This leads to applying the 20mm element size in the computations to achieve high accuracy and minimum computational time.

Table 3.3 Comparison of the mean errors of eigenfrequencies between finite elemet model with analtical results for bottom cabinet acoustic cavity in different element sizes.

Mode (l,m,n)	Error% element size 100mm	Error% element size 50mm	Error% element size 30mm	Error% element size 20mm	Error% element size 15mm	Error% element size 10mm
(1,0,0)	1,070	0,612	0,203	0,073	0,056	0,035
(0,1,0)	0,262	0,191	0,058	0,061	0,045	0,030
(1,1,0)	1,334	0,935	0,821	0,627	0,680	0,626
(0,0,1)	4,399	3,559	2,733	2,084	1,972	1,892
(1,0,1)	3,627	2,298	1,477	0,447	0,296	0,202
(0,1,1)	3,554	2,872	1,819	1,289	1,075	0,932
(1,1,1)	1,859	1,797	0,629	0,085	0,380	0,300
Error %	2,301	1,752	1,106	0,667	0,643	0,574

CHAPTER IV

EXPERIMENTAL STUDIES

In this section, pressure response of refrigerator bottom cabinet, is measured in a reverberation chamber and these results are compared with the analytical and numerical results.

4.1 Sound Pressure Level Measurement of Refrigerator Bottom Cabinet

The tested refrigerator has a cavity in the bottom cabinet as 0.6m, 0.3m and 0.25m dimensions that is excited by a compressor. Figure 4.1 shows the tested refrigerator.

Figure 4.1 The tested refrigerator

The microphone, which is used in test, is B&K 49493, ½ inches diffuse field type. Figure 4.2 shows B&K 49493 microphone. Figure 4.3 shows the technical specification of B&K 49493 microphone [29].

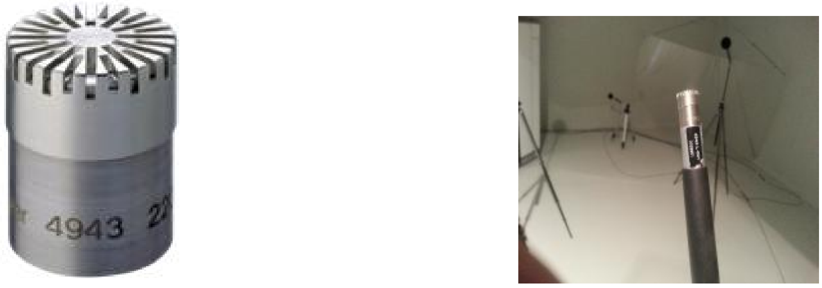

Figure 4.2 The ½-inch diffuse field microphone that is used in measurement

These microphones are called random-incidence microphones that are designed to have a uniform response when signals arrive simultaneously from all angles. They are not only used for measurement in reverberation chambers, but in all situations where the sound field is diffused, or where several sources are contributing to the sound pressure at the measurement position [29]. Practical examples are indoor situations, where the sound is reflected by walls, ceilings, and objects in the room or measurements inside a car.

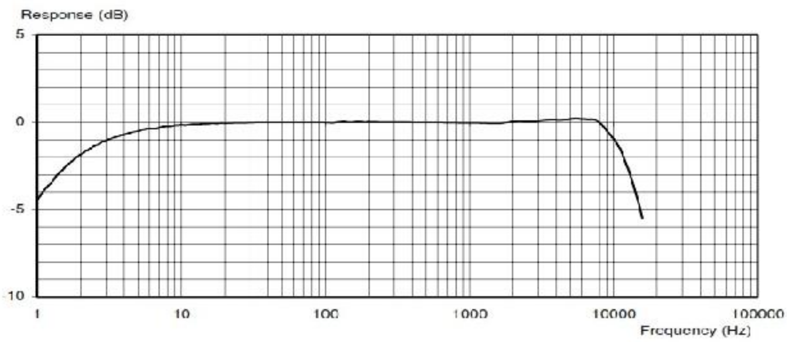

Specifications – Diffuse-field ½-inch Microphone Type 4943

Typical Use: Diffuse field measurements
Nominal Diameter: ½"
Open Circuit Sensitivity (250 Hz)*: –26 ±2 dB re 1 V/Pa, 50 mV/Pa
Polarization Voltage: 200 V external
Random-incidence Response*:
±1 dB, 5 Hz to 6.3 kHz
±2 dB, 3.15 Hz to 10 kHz
Lower Limiting Frequency (–3 dB): 1 Hz to 2 Hz
Pressure Equalization Vent: Rear vented
Diaphragm Resonance Frequency: 12 kHz (90° phase-shift)
Capacitance (Polarized)*: 20 pF at 250 Hz
Equivalent Air Volume: 36 mm^3 (250 Hz)
Cartridge Thermal Noise: 15.5 dB(A) 16.2 dB (Lin)
Upper Limit of Dynamic Range (3% Distortion): >148 dB SPL
Maximum Sound Pressure Level: 159 dB (peak)

Environmental

Operating Temperature Range: –40 to 150°C (–40 to 302°F)
Storage Temperature:
In Case: –30 to +70°C (–22 to 158°F)
With Data Disk: 5 to 50°C (41 to 122°F)

*individually calibrated

Temperature Coefficient (250 Hz): –0.010 dB/°C (–10 to 50°C, 14 to 122°F)
Pressure Coefficient: –0.008 dB/kPa, typical
Operating Humidity Range: 0 to 100% RH (without condensation)
Influence of Humidity: <0.1 dB in the absence of condensation
Vibration Sensitivity (<1000 Hz): 62.5 dB equivalent SPL for 1 m/s^2 axial vibration
Magnetic Field Sensitivity: 4 dB SPL for 80 A/m, 50 Hz field
Estimated Long-term Stability: >1000 years/dB at 20°C (68°F), >100 hour/dB at 150°C (302°F)

Dimensions

Diameter with Grid: 13.2 mm (0.52 in)
Diameter without Grid: 12.7 mm (0.50 in)
Height with Grid: 17.6 mm (0.69 in)
Height without Grid: 16.3 mm (0.64 in)
Thread for Preamplifier Mounting: 11.7 mm – 60UNS
Note: All values are typical at 23°C (73.4°F), 101.3 kPa and 50% RH, unless measurement uncertainty or tolerance field is specified. All uncertainty values are specified at 2σ (i.e., expanded uncertainty using a coverage factor of 2)

CE compliance with EMC Directive

Figure 4.3 Specifications of microphone that is used in measurement

The B&K3039 data analyzer and PULSE signal analysis software are used in the tests. The B&K3039 has 6 channels BNC, 6 channels LEMO are used during measurements. Figure 4.4 shows B&K3039 data analyzer.

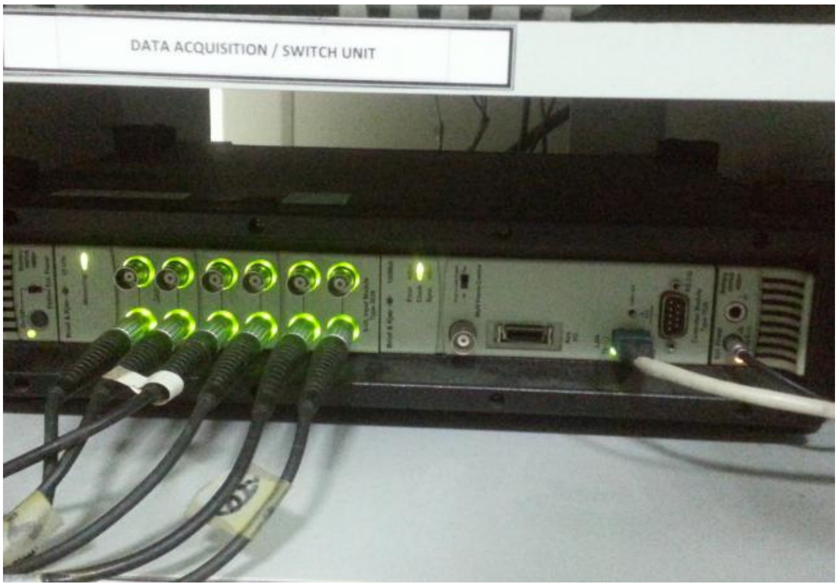

Figure 4.4 The data analyzer that is used in measurement

The test is done in a reverberation chamber, which is compatible with IEC3741. Figure 4.5 shows the reverberation chamber. The reverberation time is nearly 6 seconds and background noise is 19 dBA.

Figure 4.5 Reverberation chamber where measurement is done

A microphone is placed inside of the bottom cabinet acoustic cavity. Figure 4.6 shows the microphone position in the measurement. Sound pressure level is measured for 300 seconds; measurement graphic was generated by 3200 FFT line and processed using Hanning function. Figure 4.7 shows the pressure response of bottom cabinet cavity in frequency spectrum, which is excited by a compressor.

.

Figure 4.6 Microphone position in pressure measurement

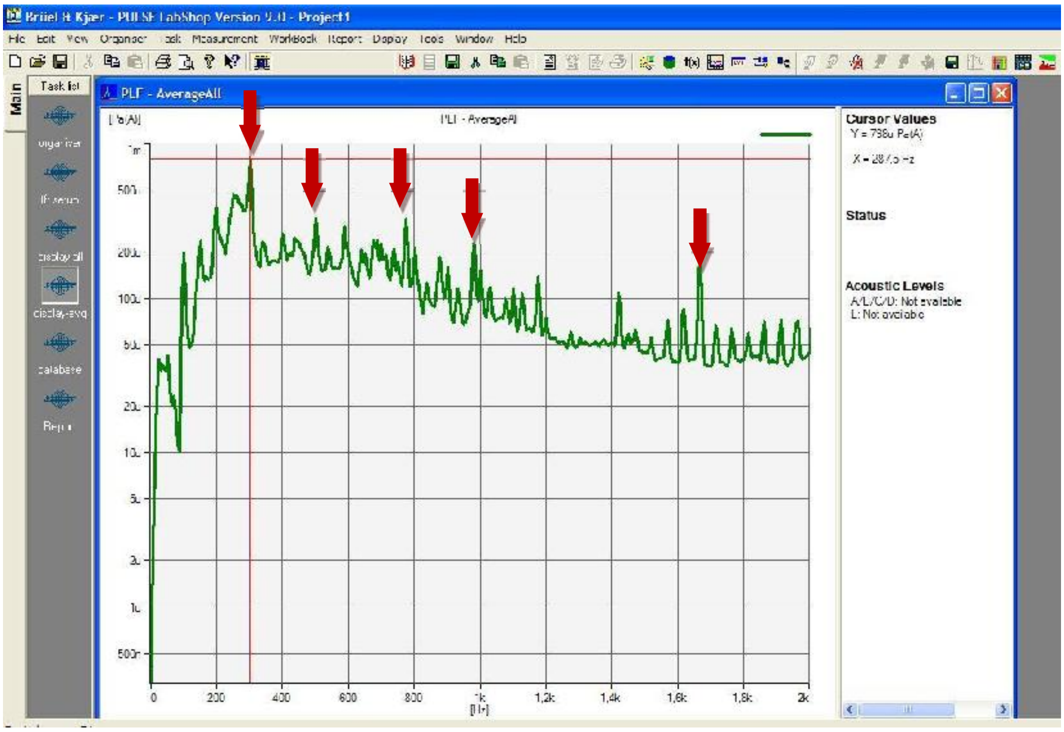

Figure 4.7 Sound Pressure Measurement Result of Bottom Cabinet Cavity

Figure 4.7 is examined, it is obviously seen that some of frequencies have high magnitude pressure level that signed respectively; (o), (p), (r), (s), (t). Table 4.1 lists some of these peak frequencies. Figure 4.8 shows also some of these peak frequencies.

Table 4.1 Peak Frequencies (Hz) of the bottom cabinet acoustic cavity which is excited by a compressor with Experimental Study

Figure Description	Frequency
(o)	287,5
(p)	596,5
(r)	762,5
(s)	982
(t)	1669

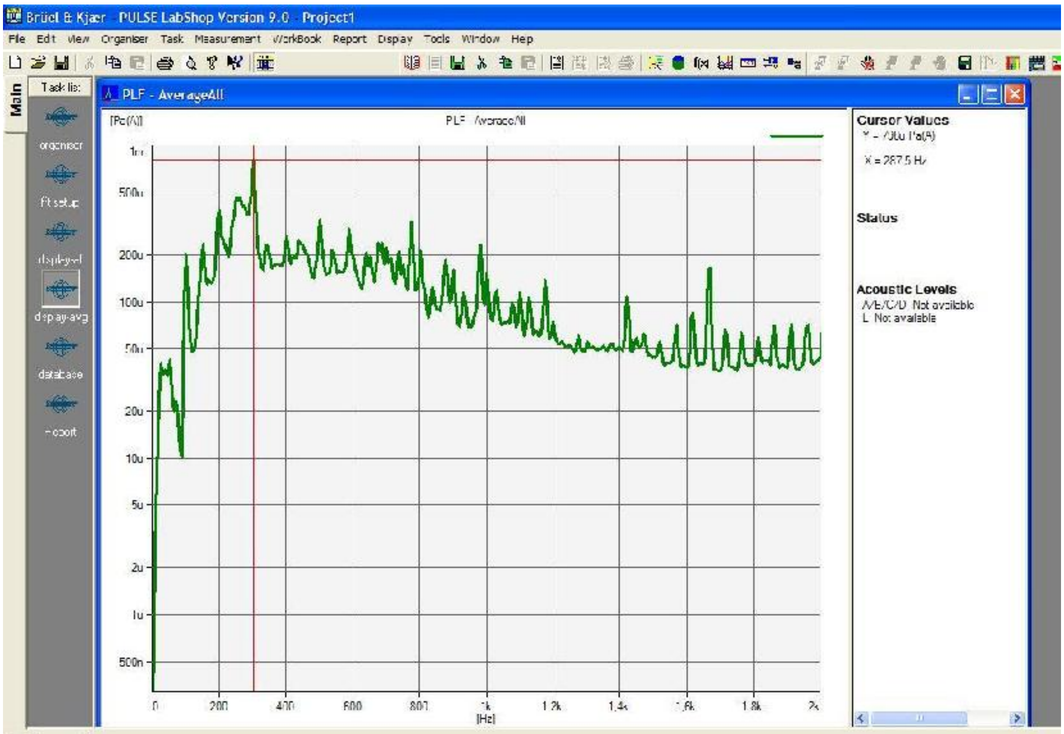

(o): 287,5 Hz

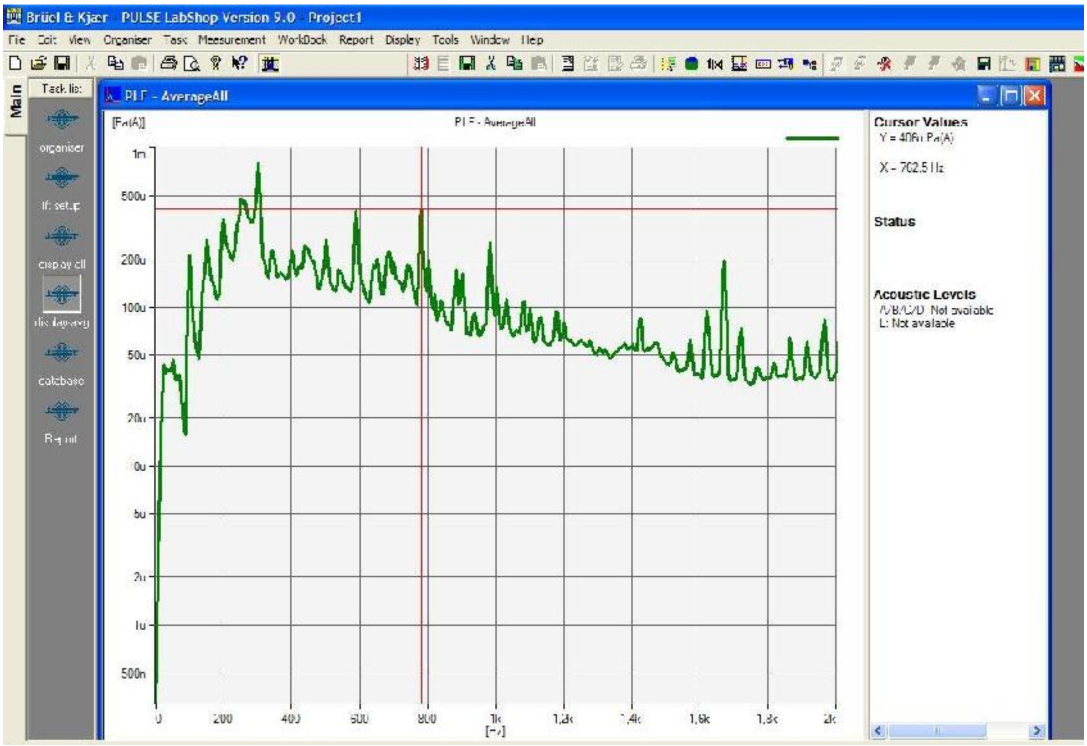

(r) : 762,5 Hz

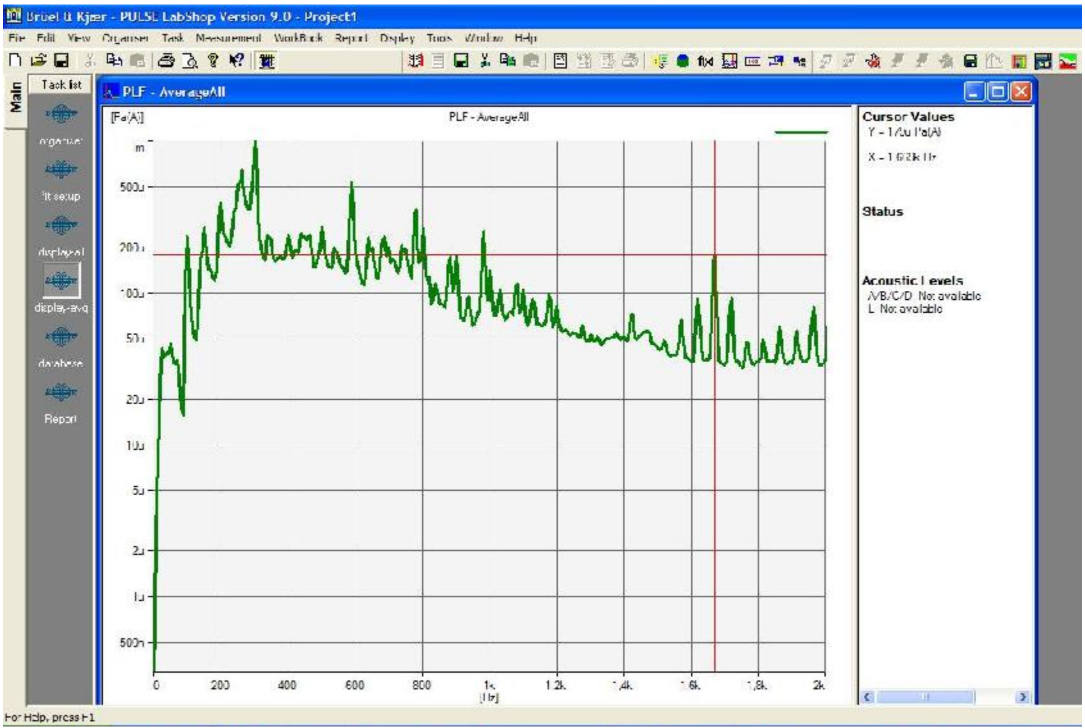

(t) :1669 Hz

Figure 4.8 A few experimental peak frequencies of bottom cabinet cavity in 287,5-762,5 and 1669 Hz

4.2 Model Verification with Results of Experimental Study

In this section, pressure response of the refrigerator bottom cabinet cavity that has peak pressure levels produced by excitation of compressor are compared with results, which are obtained with the finite element and analytical analysis. Table 4.2 lists the comparison eigenfrequency analysis between numerical, analytical and experimental for peak points that are marked in Figure 4.7.

Table 4.2 Comparison eigenfrequency analysis between numerical,analytical and experimental results for peak pressure level.

Mode (l.m.n)	Analytical	Numerical	Experimental	FEM Error versus Analytical%	FEM Error versus Experimental%
(1,0,0)	285,88	285,67	287,5	0,073	0,64
(0,1,0)	571,77	571,42	596,5	0,061	4,389
(1,0,1)	743,3	746,62	762,5	0,446	2,126
(1,1,1)	937,77	938,57	982	0,085	4,627
(1,0,3)	1716,26	1700,32	1669	1,052	1,842
	Error %			0,435	2,724

CHAPTER V

DISCUSSION

In this thesis, the finite element analysis of bottom cabinet cavity in a refrigerator is investigated. The natural frequencies of the bottom cabinet cavity are calculated with analytical study and numerical solution, respectively. Comparisons with the results of the analytical study verify the validity of the numerical solution. It is seen that finite element model of the bottom cabinet cavity is applicable. Table 3.2 lists the natural frequencies of the analytical study and numerical solution. Figure 3.8 shows the mode shapes of the analytical study and numerical solution. According to these comparisons, FEM model obviously correspond to analytical model with a mean error of 0,667%.

In this thesis, the sound pressure measurement for the response of bottom cabinet is also done experimentally, where the pressure wave source is represented by a compressor inside the cavity. It is seen that the sound pressure of the bottom cabinet of the refrigerator is higher at some frequencies. The level of sound increases at the peak frequencies. Table 4.2 lists comparison of peak frequencies between numerical, analytical and experimental studies. As a result, these frequencies are in close match with the natural frequencies of the bottom cabinet cavity of refrigerator, which are determined with the analytical and numerical analysis. FEM model correspond to experimental study with a mean error of 2,724%. The results indicate that finite element method with ABAQUS software is able to predict the natural frequency of whole modes, such that it is possible to control noise by improving acoustic behavior of rectangular cube shaped bottom cabinet cavity. Besides improving the sound comfort, modeling and characterizing the acoustic behavior of bottom cabinet cavity system is important for controlling the development cost. In this way, components in the bottom cabinet cavity would be placed according to mode shapes during prototype development.

CHAPTER VI

CONCLUSION

The noise problem in a refrigerator, in terms of the bottom cabinet cavity where compressor operates, is analyzed by using finite element method and acoustic modal analysis. To achieve accuracy on results for the bottom cabinet cavity, a relatively fine mesh is considered for the finite element computation. The following conclusions may be drawn from the results of analytical, numerical and experimental methods in this study.

- The natural frequencies of the bottom cabinet cavity are related to its dimensions.
- The bottom cabinet cavity of the refrigerator has a profound significance on the refrigerator's overall noise.
- The mode shapes of the bottom cabinet cavity are not related to its dimensions. Bottom cabinet cavity displays complex mode shapes at higher frequencies.
- The sound level of the refrigerator is significantly related to the natural frequency of the bottom cabinet cavity.
- The noise level increases at the peak frequencies, which belong to the bottom cabinet cavity.
- Decreasing of the sound level of the bottom cabinet cavity of the refrigerator is important in order to avoid or minimize unwanted noise conditions, such as high-pressure levels at cavity peak frequencies.

CHAPTER VII

FUTURE STUDY

In this thesis, the natural frequencies of the bottom cabinet cavity are investigated. The analytical and numerical studies are verified by experimental studies.

The following future studies may be performed for continuing the investigation presented in this thesis;

- The effects of width, depth and height of bottom cabinet cavity on the natural frequency of the bottom cabinet cavity could be investigated.

- The effect of the shape of bottom cabinet cavity on the natural frequency of the bottom cabinet cavity could be investigated.

- The effect of using sound absorber materials in the bottom cabinet cavity on the noise control could be investigated.

REFERENCES

[1] Directive 2010/30/EU of the European Parliament and of the Council of 19 May 2010 on the indication by labelling and standard product information of the consumption of energy and other resources by energy-related products, *Office Journal of the European Union*, (2011).

[2] R. Radermacher, Y. Hwang, *Vapor Compression Heat Pumps with Refrigerant Mixtures*, Taylor & Francis Group, 2005.

[3] Refrigerator Circuit, *Embraco Company Presentation, (2011).*

[4] Centrifugal compact fan for NoFrost system means no need for manual defrosting, *Ebm Papst NoFrost cooling*, (2010).

[5] Hermetic Compressor Service Handbook, *Tecumseh Product Company*, (2011).

[6] Refrigeration Devices Business Unit, *Panasonic Corporation Presentation*, (2012).

[7] W. Neise, Application of similarity laws to the blade passage sound of centrifugal fans, *Journal of Sound and Vibration*, 43(1), 61-75, (1975).

[8] W. Neise, Noise reduction in centrifugal fans: a literature survey, *Journal of Sound and Vibration*, 45(3), 375-403, (1976).

[9] W. Neise, Review of noise reduction methods for centrifugal fans, *Journal of Engineering for Industry*, 104, 151-161, (1982).

[10] S. Velarde-Suárez, R. Tajadura, J.B. Cruz, C. Morros, Experimental determination of the tonal noise sources in a centrifugal fan, *Journal of Sound and Vibration*, 295, (2006).

[11] S. Velarde-Suárez, et al., Reduction of the aerodynamic tonal noise of a forward-curved centrifugal fan by modification of the volute tongue geometry, *Applied Acoustics*, 69, 225-232, (2008).

[12] D. Deveci, O.Çelikkan, E.Şafak, H. Erol, Study on the noise of freezer fan, *International Congress on Sound and Vibration*, Bangkok, Thailand (2013).

[13] J. Ryu, C. Cheong, S. Kim, S. Lee, Computation of internal aerodynamic noise from a quick-opening throttle valve using frequency-domain acoustic analogy, *Applied Acoustics*, 66, 1278-1308, (2005).

[14] S. Lee, S. Heo, C. Cheong, Computation of Internal Aeroacoustics of Centrifugal Fan for Icing in Refrigerator, *15th International Congress of Sound and Vibration*, Daejeon, Korea, (2008).

[15] S. Lee, S. Heo, C. Cheong, Computation of Internal Aeroacoustics of Axial Freezing Fan in Refrigerators, *37th Internoise 2008,* Shanghai, China, (2008).

[16] H. Tanaka, K. Ishjima, K. Asami, Noise and Efficiency of Rolling, Piston, Type, Refrigeration Compressor for Household Refrigerator and Freezer, *Proc of Compressor Tech. Conf*, p.133, (1980).

[17] H. Tanaka, K. Ishjima, K. Asami, Improvements in Compressors with Special Emphasis on Interesting Developments in Japan, *Proc of Compressor Tech. Conf.*, p.268, (1982).

[18] S. Shimode, K.Ikawa, Cavity Resonance in Annular Cavity, *The Journal of the Acoustical Society of Japan*, (1977).

[19] M.C.C. Tsao, On the Mechanism of Noise by a Hermetic Reciprocating Compressor with Reed Valves, *Symposium of Noise and Fluid Engineering*, (1977).

[20] K. Tojo, S. Machida, S. Saegusa, T. Hirata, Noise Reduction of Refrigerator Compressors, *International Compressor Engineering Conference*. Paper 338, (1980).

[21] A.L. Klosterman, R. Lemon, Dynamic Analysis of Coupled Structures Using Experimental Data, *ASME Vibration Conf*., April (1969).

[22] T.E. Rook, Modeling of the Bottom Cover Dynamics of a Scroll Compressor, *International Compressor Engineering Conference*, Paper 1174, (1996).

[23] R.J. Comparin, Vibration Isolation for Noise Control in Residential Condensing Units, *Proc Int. Compressor Conf.*, Paper 265 (1994).

[24] Wang Ning, JinTao, Compressor Refrigerator Down Thtoat Finite Element Vibration Simulation, *Zhejiang University*,(2005).

[25] R.J. Wilson, Compressor Noise Control in Applications, *International Compressor Engineering Conference*, Paper 122, (1974).

[26] N. Tsujiuchi, T. Koizumi, S. Usui, K. Tsukiori, Vibration and Noise Reduction of Household Refrigerator Using Modal Component Synthesis Technique, *International Compressor Engineering Conference*, Paper 640, (1988).

[27] G. Buligan, M.D. Libera, A.D. Prampero, M. Lamantia, A. Pezzutto, Shell Optimisation Through Vibro-Acoustic Analysis, *International Compressor Engineering Conference*, Paper 1561, (2002).

[28] L.E. Kinsler, A.R. Frey, A.B. Coppens, J.V. Sanders, *Fundamentals of Acoustics 4th*, Cavities and Waveguides, P. 246, John Wiley & Sons, 2000.

[29] Type 4943 ½ inch diffuse field microphone, *Brüel & Kjær Sound and Vibration Measurement Web Portal*.

VITA

Anıl Öztürk was born in Artova, Tokat, on July 22, 1986. After completing his degree at Milli Piyango Anatolian High School, İzmir, in 2004, he entered Celal Bayar University at Manisa, receiving the degree of Bachelor of Science in Mechanical Engineering in July, 2008. For the next 18 months, he pursued a career in construction equipment machinery, doing new projects for hydraulics systems of heavy equipment in İzmir. He has been working as an acoustic engineer in Vestel White Appliances Refrigerator Factory since November 2010.

Permanent Contact Address: anilztrk@gmail.com